Nuclear Inst. and Methods in Physics Research, A 981 (2020) 164491

Contents lists available at ScienceDirect

Nuclear Inst. and Methods in Physics Research, A

journal homepage: www.elsevier.com/locate/nima

First results of the TIMESPOT project on developments on fast sensors for future vertex detectors

A. Lai [a,*], L. Anderlini [b], M. Aresti [a], A. Bizzeti [b,c], A. Cardini [a], G.-F. Dalla Betta [d,e], G.T. Forcolin [d,e], M. Garau [a,f], A. Lampis [a,f], A. Loi [a,f], C. Lucarelli [b,g], R. Mendicino [d,e], R. Mulargia [h,i], M. Obertino [j,k], E. Robutti [h,i], S. Vecchi [l]

[a] INFN Sezione di Cagliari, Strada provinciale per Sestu, Km 1, I-09042 Monserrato (CA), Italy
[b] INFN Sezione di Firenze, Via G. Sansone, 1, 50019 Sesto Fiorentino (FI), Italy
[c] University of Modena e Reggio, Dipartimento di Fisica, via G. Campi, 213/A, Modena, Italy
[d] University of Trento, Dipartimento di Ingegneria Industriale, Via Sommarive 14, I-38123 Trento, Italy
[e] TIFPA INFN, Via Sommarive 14, I-38123 Trento, Italy
[f] University of Cagliari, Dipartimento di Fisica, Strada provinciale per Sestu, Km 1, I-09042 Monserrato (CA), Italy
[g] University of Firenze, Via G. Sansone, 1, 50019 Sesto Fiorentino (FI), Italy
[h] University of Genova, Via Dodecanneso 33, I-16146, Genova (GE), Italy
[i] INFN Sezione di Genova, Via Dodecanneso 33, I-16146, Genova (GE), Italy
[j] University of Torino, Via P. Giuria, 1, I-10125, Torino (TO), Italy
[k] INFN Sezione di Torino, Via P. Giuria, 1, I-10125, Torino (TO), Italy
[l] INFN Sezione di Ferrara, Via Saragat 1, I-44122 Ferrara, Italy

ARTICLE INFO

MSC:
00-01
99-00

Keywords:
Fast timing
Silicon pixel with timing
High time resolution

ABSTRACT

The TIMESPOT project aims at the construction of a mini-tracker demonstrator implementing both high space and time resolutions at the single pixel level. The pixels have a pitch of 55 × 55 μm^2. Specified time resolution is equal or better than 50 ps. Developed sensors are based both on 3D silicon and diamond technologies, whose layout and fabrication process have been suitably optimized for best time resolution. Read-out pixel electronics is being developed in 28-nm CMOS technology. The first batch of 3D silicon sensors, containing several test structures based on different geometries of the electrodes, has been delivered in June 2019 and has been tested against its timing performance both under laser and minimum ionizing particle beams. In the present paper, the output of these starting measurements is presented. The sensors show very good timing performance, having σ<30 ps (sigma), although operated with non-optimized front-end electronics and in noisy environment. These results represent an important step forward in the development of pixels with timing operating at extremely high interaction rates and fluences, as required in the next generation of upgraded colliders.

1. Introduction

The requirement of time information at the pixel level in vertex detectors of future colliders can be now recognized as a well-established matter of fact. The technical challenge implied by this requirement drives the development of sensing devices having at the same time small pitch (50 μm or less), time resolutions of few tens of ps and very high resistance to particle fluences higher than 10^{16} 1 MeV neutron equivalent/cm^2 [1,2]. A corresponding adequate performance is required to front-end and readout electronics. At the present state-of-the-art, no experimental solutions exist satisfying the full set of the requirements above. The TIMESPOT project (standing for TIME and SPace real time Operating Tracker [3]) tries to attack the problem at the system level and aims at realizing a reduced-size tracker demonstrator, where all the components are designed together to reach the final goal of a tracking system with the due requirements. In particular, TIMESPOT develops 3D sensors (both in silicon and diamond) having a pitch of 55 μm. In this paper, first measurements on 3D silicon sensor are illustrated. Timing performance have been characterized both in the laboratory, under laser beam, and under particle beam at an accelerator test facility. This paper starts with a brief description on sensor design studies and on expected performance as output from simulations (Section 2). Section 3.2 describes the first characterization measurements on timing behavior realized in the laboratory. Section 3.2 discuss the results obtained in tests under Minimum Ionizing Particle beam performed at the Paul Scherrer Institute (Villigen, Switzerland). Section 4 draws the conclusions.

* Corresponding author.
E-mail address: adriano.lai@ca.infn.it (A. Lai).

https://doi.org/10.1016/j.nima.2020.164491
Received 15 March 2020; Received in revised form 27 July 2020; Accepted 27 July 2020
Available online 3 August 2020

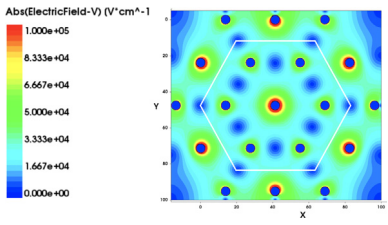

Fig. 1. Electric field map at $V_{bias} = 100$ V of a hexagonal 3D-column geometry.

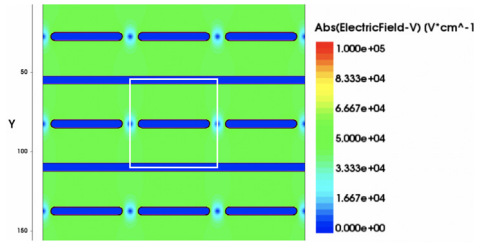

Fig. 2. Electric field map at $V_{bias} = 100$ V of a square parallel 3D-trench geometry.

2. Design of 3D sensors for timing

The initial idea of silicon sensors with vertical electrodes (3D structure) dates back to the late 90's [4]. In this type of sensors, carrier drift time can be considerably reduced, keeping a small inter-electrode (biasing and diode) distance, while the radiation absorption length is kept relatively large to provide enough charge to built-up the electronic signal. This simple and effective feature produce the advantage of naturally fast signals and enhanced radiation resistance, as the probability of defect-generated charge-trapping is reduced due to shorter drift distance of the carriers. Sensors based on 3D structures have been already found to be useful in collider experiments [5,6]. Although the signal speed of such sensors is evident by construction, 3D sensors were never fully exploited for timing and their performance in time measurements was never studied deeply. To date, only two papers [7,8] can be found reporting some preliminary measurements on time performance of 3D sensor. Although these papers give good and promising indications, a dedicated development is still lacking. We have pursued a detailed study for optimizing 3D sensors for timing. The starting point is the "classical" column structure, already used for example in ATLAS IBL [5]. Fig. 1 shows the electric field map of such a sensor at a bias voltage of 100 V, as an output of a Sentaurus TCAD simulation [9]. It can be easily argued that this electrode geometry has a basic problem concerning timing performance, due to areas having very low or even null electric field values. The effect of null-field regions cause geometric in-efficiencies which can be made negligible using the sensors in a tilted position with respect to the incident beam of particles [5]. However, they can be still important with respect to timing performance, where signal shape uniformity is a fundamental ingredient to have good time resolution. We propose a particularly homogeneous geometry, named 3D-trench geometry and illustrated in Fig. 2, which provides superior uniformity in the electric field values. Fig. 3 shows the structure of the designed 3D-trench pixel. The pixel sizes 55×55 μm^2 in area and 150 μm in depth. Pixel capacitance is in the range of 100 fF [10]. Diode (n+) electrodes are 135 μm deep and are read-out from the up surface. Bias electrodes (p+) have an ohimc contact to the bottom surface and are supplied through the support wafer (when not thinned) or through a deposited metal contact in case of thinning.

The plot in Fig. 4 gives the output of a simulation obtained with the TCODE software [11], based on a set of about 100 energy deposits from GEANT4 [12]. It provides a first indication of the timing performance of a 3D-trench structure. The different curves (and colors) refer to

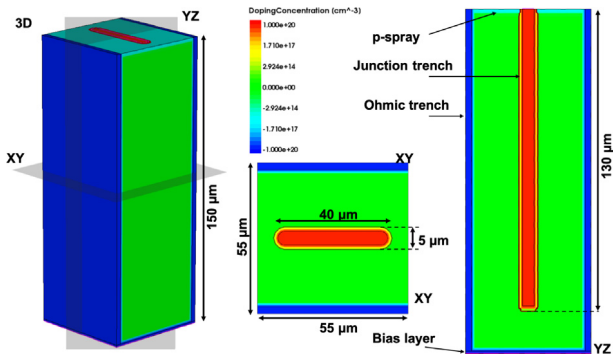

Fig. 3. Structure of the 3D-tench pixel: From left to right: 3D prospective view, XY–cut with doping level indications, YZ–cut with doping and internal structures indications.

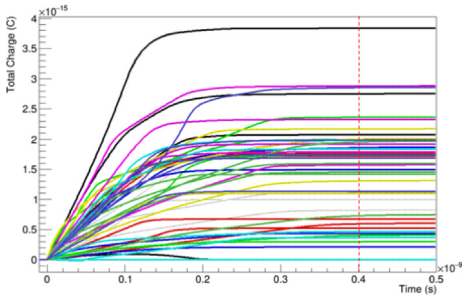

Fig. 4. Integrated charge signals at electrodes vs. time for 3D-trench pixel ($V_{bias} = -100$ V).

different minimum ionizing particle (MIP) tracks traversing the pixel with different random impact points on the surface and different angles across its volume. Charge collection is completed in less than 400 ps in the slower cases.

The first batch of 3D-trench sensors have been produced by FBK (Fondazione Bruno Kessler, Trento, Italy) and delivered in summer 2019. Details about the structure of these devices can be found in [10], where results from first measurements of I-V characteristics, breakdown voltage and pixel capacitance can be found as well. This batch contains a large variety of geometries, some of which have been chosen for first characterizations of timing performance of the 3D-trench structure and technology. The first results from tests performed on some of these pixel structures are described in the next Section.

3. Tests

The first devices selected to verify the timing performance are shown in Fig. 5. They consist of two different read-out structures, which are called *pixel-strip* and *double-pixel*. In the *pixel-strip* structure, 10 trench pixels are connected together by a metal deposit and are read-out via a single read-out pad. The *double-pixel* structure is similar, but only two pixels are connected and read-out together. As of today, no pixel read-out electronics with the right pitch and suitable timing performance exist. Therefore, these devices have been read-out by fast discrete-component front-end electronics, wire-bonded to the read-out pads of the test structures.

3.1. Tests under laser beam

First timing tests were set-up in INFN Cagliari laboratories. Here one *pixel-strip* channel was wire-bonded to a high-speed front-end board designed for diamond sensor readout by our colleagues from Kansas University (KU). A description of the board can be found in [13]. The device under test (DUT) was stimulated under laser beam. We

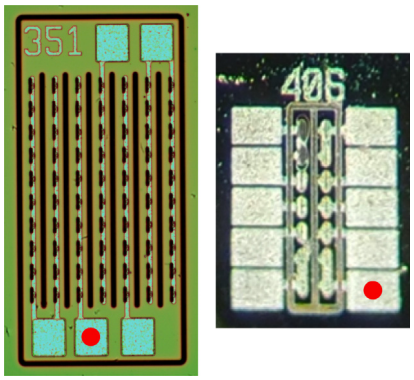

Fig. 5. Tested structures from first production batch. Left: *pixel-strip* type (10 pixels connected on the same read-out pad). Right: *double pixel* type. The red dots indicate bonding pads.

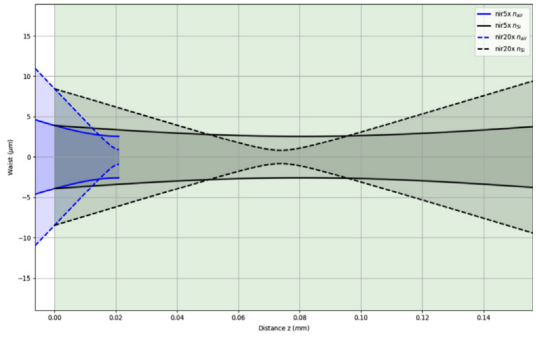

Fig. 6. Plot of the calculated 1030 nm laser waist across the sensor thickness for 5× and 20× optics. Blue shapes refer to the calculated waist in air, gray ones refer to silicon. The 5× optics provide the required cylindrical shape, mimicking a MIP-like deposit. (For interpretation of the references to color in this figure legend, the reader is referred to the web version of this article.)

used a 1030 nm, 40 MHz pulsed laser, having a pulse width of about 100 fs. A pulse-picker device allowed selecting pulses from the 40 MHz train, from full repetition rate to single pulse. The laser beam was brought to the DUT using mono-mode fibers. Optical filters were used to fix the light intensity on the DUT. The amount of deposited charge was established by previous calibration of the measured signal amplitude using a reference charge sensitive amplifier. By suitable choice of the optics setup, a laser beam with cylindrical shape and diameter of approximately 5 μm was obtained (Figs. 6 and 7). Such a beam geometry mimics the shape of a MIP charge deposit inside the sensor volume. This setup was used to measure the time delay between two subsequent laser pulses detected by the 3D-trench *pixel-strip* structure using a high-performance oscilloscope (20 Gsamples/s and 8 GHz analogue BW).

The plot in Fig. 8 shows the measurement results, giving the time resolution (sigma) of the delay as a function of the deposited charge. It is worth noticing that the time resolution corresponding to the charge delivered by a minimum ionizing particle is in the range of 20 ps. This first measurement is still only indicative but confirms the enhanced timing performance of the TIMESPOT 3D-trench device. The result is even more encouraging, considering the larger capacitance of the read-out channel, which in this device (*pixel-strip*) is approximately a factor 10 larger (corresponding to ≈ 1.5 pF).

3.2. Tests under particle beam

The crucial measurement on timing response of our 3D-trench sensors was done under a beam of minimum ionizing particles (MIP's).

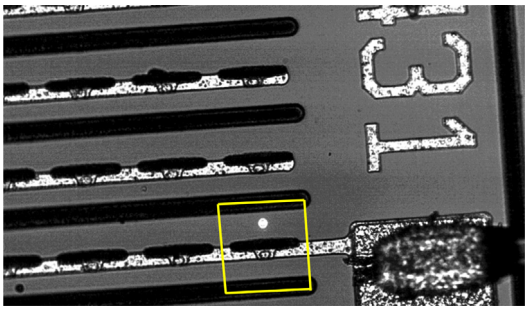

Fig. 7. Picture of a *pixel-strip* device taken by the camera of the laser-positioning microscope. The stimulating laser spot is clearly visible, allowing to appreciate its size with respect to the pixel area of 55 × 55 μm^2 (yellow square).

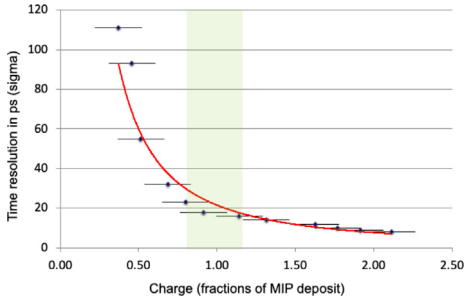

Fig. 8. Time resolution under pulsed and calibrated laser beam as a function of signal charge. Charge is expressed in fractions of Most Probable Value (MPV) of the amount delivered by a Minimum Ionizing Particle (MIP) in a silicon thickness of 150 μm (≈ 2 fC). In all these measurements, $V_{bias} = -60$ V.

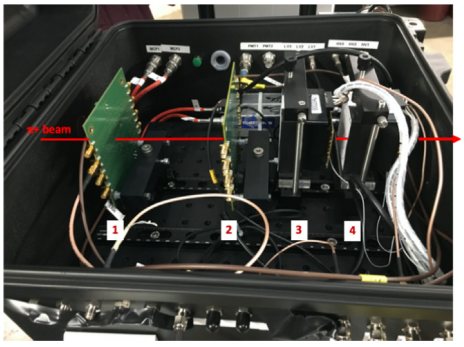

Fig. 9. Picture of test setup at PSI, πM1: (1) first device under test (DUT1); (2) second device (DUT2); (3) first Cherenkov time tagger (MCP1); second Cherenkov time tagger (MCP2).

These tests were performed in October 2019 at the beam facility πM1 [14] of the Paul Scherrer Institute (PSI) in Villigen, Switzerland.

The original πM1 beam contains a mixture of protons, positrons, positive muons and positive pions (π^+). After proper beam setup, an almost pure π^+ beam, having momentum of 270 MeV/c could be selected. At this energy, pions behave like MIPs with only an average 5% larger dE/dx deposit in silicon. The test setup is shown in Fig. 9. The π^+ beam on the spot had a radius with $\sigma \approx 1.5$ cm. Two DUTs at a time could be placed on the beam line. An accurate time reference was provided by two Micro-Channel-Plates equipped with quartz Cherenkov radiators ($\sigma \approx 15$ ps per tagger). Data were acquired by a high-end Rohde–Schwartz oscilloscope (20 Gsample/s and 8 GHz analogue bandwidth). Two different front-end circuits were used. Some DUT's of the types given in Fig. 5 were read-out with the KU board already used for the laser tests (Section 3.1), others were read-out with a different board, already developed at INFN Genova. The "Genova board" is based on

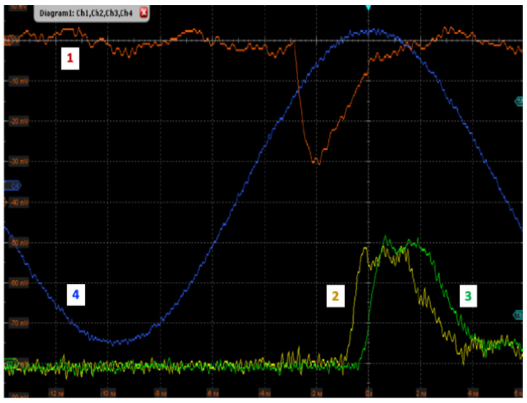

Fig. 10. Acquired waveforms from a triggered event: (1) signal from DUT1 or DUT2; (2) signal from time tagger MCP1; (3) signal from time tagger MCP2; (4) beam RF signal. Amplitude scale: 10 mV/div. Time scale: 1 ns/div.

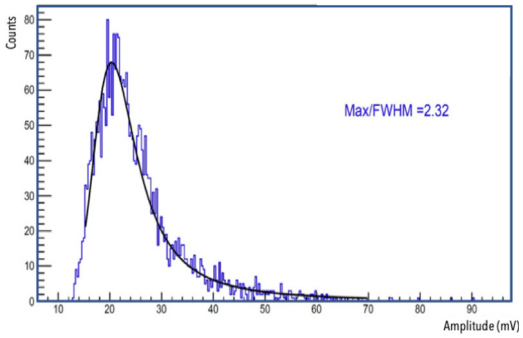

Fig. 11. Amplitude distribution of the signals from the tested sensor (double pixel type). The most probable value corresponds to about 2 fC. The sensor has $V_{\text{bias}} = -80$ V.

a two-stage signal amplification scheme acting as an inverting trans-impedance amplifier, implemented on a custom-made circuit. The first amplification stage is performed by an AC-coupled silicon–germanium bipolar transistor designed for high bandwidth (up to 5 GHz) and low noise applications, featuring a gain of nearly 30 dB at 2 GHz and an integrated output noise of 260 μV.

The acquisition trigger was given by the coincidence of a signal from the selected DUT and the two signals from time taggers (MCP1 and MCP2). On a trigger, four waveforms were acquired, corresponding to the three triggering signals and the beam RF signal (50 MHz), whose phase could be useful for checks about the time of flight (and identification) of the beam particles. The waveforms of a typical event are shown in Fig. 10.

As a validity check on acquired data, we first verified the shape of the amplitude distribution, which has to correspond to the proper Landau distribution for this specific silicon thickness. The distribution of the amplitudes of the signals from the silicon sensor (*double-pixel* type) is given in Fig. 11. The fit on the distribution is given by the convolution of a Landau function, a Gaussian function (to take into account the effect of electronic noise) and a step-error function, used to consider the effect of the trigger threshold on the acquiring oscilloscope. The fitting curve has a shape which is fully compatible with the absorption thickness of the sensor under test, as can be seen on [15]. This check ensures that the acquired data-set effectively counts the MIP's interacting in the sensor volume.

The time measurement consisted in determining the time delay Δt_s between the avarage time of the two time taggers $t_{MCP} = (t_{MCP2} + t_{MCP1})/2$ and the sensor signal, that is

$$\Delta t_s = (t_{\text{sensor}} - t_{\text{MCP}}). \quad (1)$$

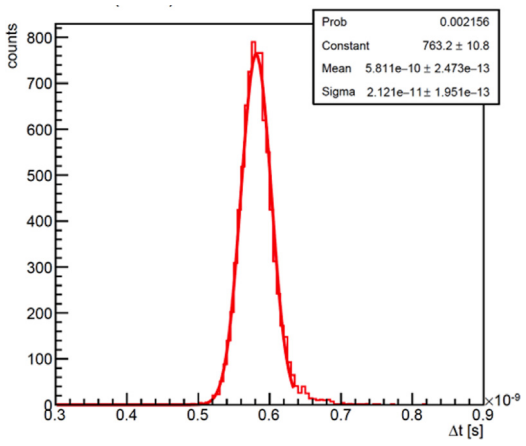

Fig. 12. Distribution of the time delay between the two time taggers, $t_{MCP2} - t_{MCP1}$. The Gaussian fit gives a distribution $\sigma = (21.2 \pm 0.2)$ ps.

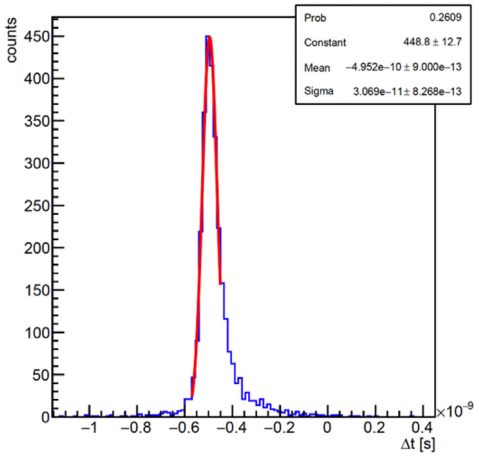

Fig. 13. Distribution of the time delay between t_{MCP} and t_{sensor}, named Δt_s, determined after application of a CFD method on the waveforms. The sensor has $V_{\text{bias}} = -80$ V.

The particle arrival times (t_{MCP1}, t_{MCP2} and t_{sensor}), were measured after proper processing of the waveforms by applying a numerical method to obtain a constant fraction discrimination (CFD), with threshold placed at 35% of the signal maximum. As a result, the t_{MCP} and finally the Δt_s were determined.

Fig. 12 gives the distribution of time delay between the two time taggers. The average time t_{MCP} (Eq. (1)) is used as a better time reference with respect to the use of one single time tagger. The distribution of the Δt_s (Fig. 13) can be fitted by a Gaussian convoluted with a suitable fraction of an exponential tail. The measured σ, obtained by the Gaussian part of the fit, gives a time resolution for Δt_s (Eq. (1)) of $\sigma_t = (30.7 \pm 0.8)$ ps. To obtain the effective contribution to σ_t due to the sensor itself, this value must be corrected separating out the contributions of the two time taggers, finally giving the value:

$$\sigma_t(@V_{\text{bias}} = -80 \text{ V}) = (28.9 \pm 0.4) \text{ ps}, \quad (2)$$

as time resolution of our 3D-trench sensor of the *double-pixel* type.

The non-Gaussian tail of the distribution is given by slower signals and can be interpreted as a combination of the following contribution:

- Failure of the CFD algorithm due to irregular/noisy signals;
- In-time spurious signals due to EMI noise (ringing), which was particularly high, especially due to discharges of the MCP's;
- Border effects due to the impossibility of clustering corrections (owing to the isolated pixel read-out);

Table 1
Qualitative comparison of time resolutions obtained in different sensor-electronics setups.

Test structure	Front-end type	σ_t (ps)
Pixel strip	KU (unshielded)	40–50
Single pixel	KU (unshielded)	35
Hexagonal column	KU (unshielded)	60–70
Double pixel	INFN GE (shielded)	<30
Single pixel	INFN GE (shielded)	Oscillations
ATLAS Ph2 (poly connect.)	KU (unshielded)	>100

- Residual weak electric field spots in the sensitive pixel volume (e.g.inter-electrode areas).

The detailed structure of the tails is still under study. However, as a worst-case scenario, should also be the observed tail an intrinsic feature of the time response, it is practically negligible when such sensors are used in a tracking system, in coincidence with multiple tracking planes of the detector.

During the test-beam, we also performed several other measurement on different sensor structures coupled with two different front-end electronics. For a quick and only qualitative comparison, they are summarized in Table 1.

This table is useful to highlight the strong dependence of our timing measurements on the specific electronics used. Indeed, the read-out electronics available to us was still not optimized for our sensors. Moreover, wire-bonding connections caused a sensible worsening of the performance, due to increased capacitance and electromagnetic pick-up. Our TIMESPOT team is presently developing its own dedicated electronics (both discrete-components and integrated) which will be soon used in our test campaigns. On the other hand, the excellent timing performance obtained even without optimized front-end, demonstrate that 3D-trench silicon sensors are really robust in their timing behavior.

4. Conclusion

3D silicon trench sensors are being developed to investigate if they can meet the stringent requirements on position and timing resolution, as well as radiation resistance required by future high energy physics experiments. The first batch of 3D-trench devices, designed and optimized by simulation for enhanced timing capabilities, has been completed. They have been tested in the laboratory under laser beam, obtaining time resolutions in the range of 20–30 ps. This preliminary result was soon confirmed under beam of charged pions, having momentum of 270 MeV/c, that is in conditions similar to those to be found at a particle collider. The measured time resolution in this case has been measured below 30 ps. A more refined analysis of test-beam data is ongoing. Tests and data analysis on the various test structures produced are being pursued to fully characterize this type of sensors, which can be very effective for experiments at the next generation of colliders.

Declaration of competing interest

The authors declare that they have no known competing financial interests or personal relationships that could have appeared to influence the work reported in this paper.

Acknowledgments

This work was supported by the Italian National Institute for Nuclear Physics (INFN), 5th Scientific Commission (CSN5), Project TIMESPOT and by the ATTRACT-EU initiative, INSTANT project.

References

[1] LHCb Collaboration, Expression of Interest for a Phase-II LHCb Upgrade: Opportunities in flavour physics, and beyond, in the HL-LHC era, CERN-LHCC-2017-003.
[2] FCC Collaboration, The Future Circular Collider (FCC) Conceptual Design Report, CERN-ACC-2018-0057, CERN-ACC-2018-0058, CERN-ACC-2018-0059.
[3] TIMESPOT web site: https://web.infn.it/timespot/index.php.
[4] S.I. Parker, et al., A proposed new architecture for solid-state radiation detectors, Nucl. Instrum. Methods A 395 (3) (1997) 328.
[5] B. Abbot, et al., (The ATLAS IBL Collaboration), Production and integration of the ATLAS insertable B-layer, JINST 13 (2018) T05008.
[6] F. Ravera, (The CMS Collaboration), The CT-PPS tracking system with 3D pixel detectors, JINST 11 (2016) C11027.
[7] S.I. Parker, et al., Increased speed: 3D silicon sensors; Fast current amplifiers, IEEE Trans. Nucl. Sci. 58 (2) (2011) 404.
[8] G. Kramberger, et al., Timing performance of small cell 3D silicon detectors, Nucl. Instrum. Methods A 934 (2019) 26.
[9] Synopsys Sentaurus TCAD software: https://www.synopsys.com/silicon/tcad.html.
[10] G.T. Forcolin, et al., 3D Trenched-Electrode Pixel Sensors: Design, Technology and initial results, in: 12th International Hiroshima Symposium on the Development and Application of Semiconductor Tracking Detectors (HSTD12).
[11] A. Contu, A. Loi, TimeSPOT COde for DEtector Simulation (TCODE): https://github.com/MultithreadCorner/Tcode.
[12] S. Agostinelli, et al., Geant4: A simulation toolkit, Nucl. Instrum. Methods A 506 (2003) 250.
[13] G. Antchev, et al., Diamond detectors for the TOTEM timing upgrade, JINST 12 (2017) P03007.
[14] PSI πM1 Beamline. https://www.psi.ch/en/sbl/pim1-beamline.
[15] S. Meroli, D. Passeri, L. Servoli, Energy loss measurement for charged particles in very thin silicon layers, JINST 6 (2011) P06013.